Cardiac remodeling and higher sensitivity to ischemia-reperfusion injury in female rats submitted to high-fat high-sucrose diet: an in vivo / ex vivo longitudinal follow-up

Natacha Fourny, Carole Lan, Frank Kober, Doria Boulghobra, Jordan Bresciani, Cyril Reboul, Monique Bernard, Martine Desrois

HAL Id: hal-02372107
https://amu.hal.science/hal-02372107

Submitted on 20 Nov 2019

Cardiac remodeling and higher sensitivity to ischemia-reperfusion injury in female rats submitted to high-fat high-sucrose diet: an *in vivo / ex vivo* longitudinal follow-up.

Natacha Fourny [a], Carole Lan [a], Frank Kober [a], Doria Boulghobra [b], Jordan Bresciani [a], Cyril Reboul [b], Monique Bernard [a] and Martine Desrois [a].

[a] Aix Marseille Univ, CNRS, CRMBM, Marseille, France

[b] Université d'Avignon, LaPEC EA4278, Avignon, France

Running title: Prediabetes and female rat heart

Corresponding author: Natacha Fourny, Phone: +33 (0) 4 91 32 48 08 / Fax: +33 (0) 4 91 25 65 39, natacha.fourny@etu.univ-amu.fr

Centre de Résonance Magnétique Biologique et Médicale (CRMBM), UMR 7339, Aix-Marseille Université, CNRS, Faculté de Médecine, 27 Boulevard Jean Moulin, 13385 Marseille Cedex 05, France.

carole.lan@univ-amu.fr ; frank.kober@univ-amu.fr ; doriaboulghobra@gmail.com ; jordan.bresciani@etu.univ-amu.fr ; cyril.reboul@univ-avignon.fr ; monique.bernard@univ-amu.fr ; martine.desrois@univ-amu.fr

Abstract

Prediabetes is an important risk factor for type 2 diabetes and cardiovascular complications, such as myocardial infarction. However, few studies explore female sex in this context. Here, we aim to investigate the effects of high-fat high-sucrose diet on cardiac parameters and sensitivity to ischemia-reperfusion injury of female Wistar rats. Female Wistar rats received for 5 months normal diet (CTRL group) or high-fat high-sucrose diet (HFS group). Every month MRI was performed to follow myocardial morphology, function and perfusion; cardiac and hepatic triglyceride content; and amount of sub-cutaneous and visceral adipose tissues. Then, *ex vivo* experiments were performed on isolated perfused hearts to evaluate tolerance to ischemia-reperfusion, with simultaneous measurement of energy metabolism by ^{31}P MRS and contractile function. Coronary flow was measured before and after ischemia. At the end of the experiments, hearts were freeze-clamped for biochemical assays. Five months of high-fat high-sucrose diet induced a prediabetic condition in female Wistar rats, associated with an increase in myocardial perfusion, systolic and diastolic wall thickness. HFS rats also exhibited higher sensitivity to ischemia-reperfusion injury in comparison to controls, characterized by impaired cardiac function, energy metabolism and endothelial function. Biochemical analyses in hearts highlighted eNOS uncoupling, higher malondialdehyde level and lower S-Glutathionylation of proteins in HFS rats, indicating higher oxidative stress. Prediabetes induced by energy-dense diet was associated with modification of cardiac morphology and higher myocardial sensitivity to ischemia-reperfusion injury. These results may be related to the high risk of cardiovascular complications among type 2 diabetic women.

Key words: Prediabetes; High-fat high-sucrose diet; Female gender; Cardiac MRI; Ischemia-reperfusion; Oxidative stress.

1. Introduction

Type 2 diabetes is worldwide recognized as a public healthcare issue affecting 425 million of people [1]. The leading cause of mortality and morbidity in type 2 diabetic patients remains cardiovascular (CV) complications. Interestingly, type 2 diabetes leads to CV complications [2] and mortality [3] more frequently in women than men. The risk of myocardial infarction is indeed 5 times higher in diabetic women than in non-diabetic women, whereas this risk increases only twice in men [2]. However, until now, only a small number of studies focus on female sex.

Prediabetes, a condition characterized by increased fasting plasma glucose and/or intolerance to glucose, is also related to an increase of type 2 diabetes and CV risk [4]. Recently, the Maastricht study showed that there are already sex differences in CV risk before the onset of type 2 diabetes, with more adverse cardiometabolic profile in prediabetic women [5]. During the transition from normoglycemia to impaired fasting glucose and type 2 diabetes, women present higher levels of endothelial factors and fibrinolytic / thrombotic factors than men, leading to greater endothelial dysfunction and insulin resistance [6]. The risk of heart and coronary disease is also higher at lower glucose levels in women [7]. Factors such as oxidative stress, inflammation, dyslipidemia and mitochondrial dysfunction can contribute to endothelial dysfunction, to microvascular and macrovascular damage, leading to CV complications [8]. Prediabetes is often associated with other risk factors of type 2 diabetes and CV diseases, such as abdominal obesity, hypertriglyceridemia, low HDL-cholesterol and raised blood pressure, clustered as metabolic syndrome (MetS) [9]. MetS is a strong predictor of the onset of type 2 diabetes with a higher risk of 52%. MetS could be responsible for 17% of CV events and 7 % of death by CV disease [10] and contributes to the increase by 78% of CV risk and death in MetS patients [11]. Therefore, more studies are needed to better understand prediabetic and metabolic syndrome conditions leading to higher CV risk in type 2 diabetes, particularly in women. As prediabetes and metabolic syndrome are strongly associated with obesity [12], it becomes clear that our environment and life habits play an important role in the disease pathogenesis. The increased intake of western diet and the decrease of physical activity combined with genetic predisposition have strongly contributed to appearance and spreading of MetS [13].Thus, energy-dense-diet-induced animal model could help us explore CV complications of prediabetes and MetS conditions.

The first objective of our study was to investigate the effect of a high-fat high-sucrose diet on cardiac morphology and function in parallel to the development of prediabetes in female rats, with a longitudinal follow-up *in vivo* using magnetic resonance imaging (MRI) and spectroscopy (MRS). The second objective was to assess the impact of high-fat high-sucrose diet on the sensitivity of heart during an ischemia-reperfusion injury, in which we combined measurement of myocardial and endothelial function with simultaneous evaluation of energy metabolism using ^{31}P MRS. Finally, at the end of the experiments, we have explored cellular integrity, nitric oxide (NO) pathway, apoptosis and oxidative stress in the myocardial tissue to probe further into the molecular mechanisms induced by high-fat high-sucrose diet. To our knowledge, this is the first study to consider cardiac longitudinal follow-up and tolerance to

ischemic insult in prediabetic female rats under high-fat high-sucrose diet, using MRI and MRS combined with biochemical analyses.

2. <u>Materials and Methods</u>

For details, see Supplementary Material.

2.1 Animal model

Seven-week-old female Wistar rats (around 170 g, Charles River, France) (n=20) were housed in a ventilated rack cabinet, with controlled temperature (22-24°C) and multiple environmental enrichments. All procedures involving animals were approved by the Animal experiment ethic committee of the University (APAFIS#10547-2017071009112930) and were performed in conformity with the Directive 2010/63/EU of the European Parliament on the protection of animals used for scientific purposes. Animals had access to food and water *ad libitum.* Female Wistar rats were divided randomly in two groups of 10: The control group (CTRL) was fed with standard diet (SAFE, A04C-10); and the HFS group was fed with high-fat high-sucrose diet (SAFE, U8978 v19; composition detailed in Table 1). Rats received diets for five months, and weight and food intake were measured every week. Food efficiency was calculated as the ratio of weight gain on food intake over the 5 months of diet.

2.2 Study design

The experimental protocol is summarized in Figure 1. At 7 weeks of age, twenty female rats underwent an initial MRI/MRS investigation (T0). They were randomized into two groups (CTRL and HFS), and an MRI/MRS exam was performed on all rats every month. After 5 months of diet, they underwent an intraperitoneal glucose tolerance test (IPGTT) to evaluate their metabolic status, and arterial blood pressure (BP) was measured. After sacrificing the animals, *ex vivo* experiments on isolated perfused heart were performed to assess myocardial function and tolerance to ischemia-reperfusion injury. At the end of the experiments, hearts were freeze-clamped for biochemical analyses.

2.3 Magnetic Resonance Imaging (MRI) and Spectroscopy (MRS) investigations

The MRI and MRS examinations were performed to evaluate *in vivo* cardiac morphology, cardiac function, myocardial perfusion, cardiac and hepatic triglycerides (TG) content and the amount of visceral (VAT) and subcutaneous (SCAT) adipose tissue in the body. All

acquisitions were performed using a Bruker Biospec Avance MR system equipped with a 4.7 Tesla magnet (Bruker, Ettlingen, Germany) and a proton volume resonator (diameter 60 mm; homogeneous length 80 mm).

Before the experiments, rats were sedated by inhalation of 3.5% isoflurane. During MRI/MRS investigations, anesthesia was maintained at 1.5-2.5% isoflurane in 1 L/min pure oxygen-flow to obtain regular breathing at a rate of around 70 breaths per minute. Respiration, ECG signal and temperature were monitored during the whole procedure.

Every month, an ECG-gated gradient-echo cine-MRI sequence (cine-FLASH) was used for the assessment of myocardial mass and function [14]. *In vivo* myocardial perfusion was quantified using the Arterial Spin Labeling (ASL) technique [15]. At 5 months, cardiac and hepatic ^{1}H MR spectra were acquired for TG assessment using an ECG- and respiratory-gated Point-Resolved Spectroscopy (PRESS) sequence [16]. The TG/water signal ratio was calculated to obtain TG concentration. For a quantitative map of adipose tissue distribution, whole-body scanning was performed. Sixty-four contiguous axial imaging slices were selected across the animal body length excluding the tail [17, 18]. After each experiment, animals were kept alone under infrared light during wakefulness.

2.4 Intra-peritoneal Glucose Tolerance Test (IPGTT) and Blood Pressure assessment at T5 months

An IPGTT was performed after 6 hours of fasting to evaluate glucose homeostasis. Glycemia was measured before and 15, 30, 60, 90, 120 minutes after injection of a bolus of glucose, using ACCU-CHEK Performa Nano Glucometer (Roche, Switzerland).

BP was recorded non-invasively by the tail cuff method (Bioseb, Chaville, France) [19].

2.5 Isolated perfused heart preparation and tolerance to ischemia-reperfusion injury

Rats were anesthetized by intraperitoneal injection of 90mg/kg pentobarbital sodium. Hearts were cannulated and perfused in the Langendorff mode at constant pressure as described previously [20].

2.5.1 Experimental protocol

After stabilization, hearts were perfused for 24 minutes with a physiological Krebs-Henseleit buffer containing 0.4 mM palmitate, 3% albumin, 11 mM glucose, 3U/L insulin, 0.8 mM lactate and 0.2 mM pyruvate. Before low-flow ischemia, they were perfused with physiological Krebs-Henseleit buffer containing 1.2 mM palmitate and then underwent a low-flow ischemia (0.5 mL/min/g wet wt) of 32 minutes with the same buffer. A higher concentration of palmitate (1.2 mM) was provided during ischemia to cause maximal damage during ischemia and reperfusion [21]. Finally, flow was restored entirely for 32 minutes with the physiological Krebs-Henseleit buffer containing 0.4 mM palmitate. This protocol was previously reported to provide sufficient level of ischemia in a type 2 diabetic animal model [20].

2.5.2 Evaluation of myocardial function and energy metabolism

A water-filled latex balloon was inserted in the left ventricle to record developed left ventricular pressure (DP) and heart rate (HR) [22]. The product of DP and HR (in mmHg/min) was used as an index of myocardial function. Coronary flow (CF) was measured by collection of coronary effluent before and after ischemia (at 20 minutes and 80 minutes of protocol). CF is expressed in mL/min/g wet weight.

Energy metabolism was evaluated as previously described [23]. Briefly, perfused rat hearts were placed in a 20-mm magnetic resonance sample tube and inserted in a 4.7 Tesla magnet (Oxford instruments, Oxford, UK) interfaced with a Bruker-Nicolet Avance WP-200 spectrometer (Bruker, Karlsruhe, Germany). A series of eight ^{31}P NMR spectra were recorded during every period of the experimental protocol to quantify phosphorus metabolite signals (ATP, PCr and Pi) and intracellular pH.

2.6 Dissection and collection of samples

VAT, SCAT, tibia and blood were collected for evaluation of physiological parameters. At the end of the experiments, hearts were freeze-clamped in liquid nitrogen with a Wollenberger clamp and kept at -80°C for subsequent analysis.

2.7 Biochemical analyses

In plasma, assay kits were used to determine glucose (Randox Laboratories, Crumlin, Antrim UK), Free Fatty Acids (FFAs) (NEFA kit; Roche Diagnostics, Roche Applied Science, Mannheim, Germany), TG (Abcam, ab 65336), HDL- and LDL-Cholesterol (Abcam, ab 65390).

In freeze-clamped hearts, cellular integrity was evaluated by measurement of creatine kinase (CK) (CK-NAC, Randox Laboratories, Crumlin, UK) and lactate dehydrogenase (LDH) activities [23]; apoptosis with expression of cleaved caspase-3 by Western Blot [24]; NO pathway with the expression of total eNOS (endothelial NO synthase), P-eNOS (phosphorylated on Ser1177) and eNOS dimer-to-monomer ratio (eNOS d/m) by Western Blot [25, 26]; proteins post-translational modification with evaluation of S-Glutathionylation by Western Blot; and oxidative stress with assessment of Malondialdehyde (MDA), an index of lipid peroxidation, with the lipid peroxidation assay kit (MAK085, Sigma-Aldrich, St Louis, USA).

2.8 Expression of results and statistical analyses

Data are graphically provided as mean ± SEM of absolute values. Graph Pad Prism software 5.0 (La Jolla, CA) was used for all statistical processing. Significant differences between groups were determined using two-way analysis of variance (ANOVA) with repeated measures over time for the time-dependent variables followed by Bonferroni post-hoc test. An unpaired Student's **t**-test was used for the other parameters. Correlation analyses were also performed between imaging and other parameters. A p value of less than or equal to 0.05 was considered to indicate significant difference.

3. Results

3.1 Effect of high-fat high-sucrose diet on physiological parameters

Physiological parameters are summarized in Table 2. Food intake was significantly lower in HFS versus CTRL during the whole diet ($p<0.0001$), while calorie intake and food efficiency were significantly increased (respectively $p<0.001$ and $p<0.01$). After 5 months of diet, the weight and the lean mass of animals was not different between groups, and neither systolic or diastolic arterial blood pressure. However, fat mass percentage was significantly higher in HFS vs. CTRL. Amount of VAT and SCAT measured by MRI was significantly higher at T5 ($p=0.014$ and $p=0.01$, respectively), as well as VAT measured by dissection ($p<0.05$ vs.

CTRL; p=0.08 for SCAT) in HFS vs. CTRL. Measurement by MRI and dissection were strongly correlated (VAT, r=0.98; SCAT, r=0.90). The percentage of cardiac TG was not different between groups, but the percentage of hepatic TG was significantly higher in HFS vs. CTRL at T5 (p<0.001). Heart weight-to-tibia-length ratio was similar in both groups. Plasma FFAs and fasting plasma glucose were significantly higher in HFS compared with CTRL (p<0.05 and p<0.01 respectively). No difference was found in plasma TG and HDL-Cholesterol, but LDL-Cholesterol was significantly higher in HFS compared with CTRL (p<0.05). The IPGTT highlighted a significant glucose intolerance in HFS compared with CTRL (p<0.01).

3.2 Effect of high-fat high-sucrose diet on cardiac morphology, perfusion and function

The effects of high-fat high-sucrose diet on cardiac parameters are shown in Figure 2. The high-fat high-sucrose diet led to thickening of the myocardial wall in both diastole (p<0.01, Figure 2A) and systole (p<0.01, Figure 2B), and to increased left ventricular mass (p<0.05, Figure 2C) starting at the 3rd month of diet in HFS vs. CTRL. Myocardial perfusion (Figure 2D) was significantly increased in HFS (p<0.01) from T2 month vs. CTRL. However, the high-fat high-sucrose diet had no effect on cardiac function parameters (supplemental material) compared to CTRL.

3.3 Effect of high-fat high-sucrose diet on myocardial tolerance to ischemia-reperfusion injury

3.3.1 *Ex vivo* myocardial function and coronary flow

Myocardial function (Figure 3A) evaluated by the product of DP and HR was significantly lower in baseline conditions (p<0.05) and during reperfusion (p<0.01) in HFS vs. CTRL. The percentage of recovery, expressed as percentage of control values, was significantly lower in HFS compared with CTRL (53 % ± 6 % vs. 29 % ± 6 %; p<0.05) during reperfusion. CF was not different between groups in baseline conditions (Figure 3B). However, CF was significantly lower in HFS vs. CTRL during reperfusion (p<0.05) (Figure 3C).

3.3.2 *Ex vivo* energy metabolism and intracellular pH (pHi)

Figure 4 shows kinetics of PCr (A), ATP (B), Pi (C) and pHi (D) during the ischemia-reperfusion protocol. During the control period, no difference in PCr, ATP and Pi content was found between the two groups. During ischemia, PCr and ATP were significantly decreased in

HFS compared with CTRL (p<0.05) and Pi was similar in both groups. During reperfusion, PCr and ATP were significantly decreased, and Pi was significantly increased in HFS vs. CTRL (respectively p<0.01, p<0.05 and p<0.05). pHi was similar in both groups during the whole protocol.

3.3.3 Biochemical analyses in freeze-clamped hearts

At the end of the *ex vivo* experiments, we studied NO pathway involved in the endothelial function. The expression of total eNOS and P-eNOS (Figures 5A and 5B) was similar between CTRL and HFS. However, we found an increase of uncoupled eNOS (inactive form) in HFS, characterized by significantly lower eNOS dimer-to-monomer ratio (Figure 5C) in comparison to CTRL (p<0.01), indicating an impaired endothelial function. Total S-Glutathionylation (Figure 5D) of proteins was decreased (p=0.052) in HFS compared with CTRL, indicating a potentially diminished protection against oxidative stress. S-Glutathionylation of eNOS (Figure 5E) was similar between groups. Malondialdehyde, a lipid peroxidation marker, was significantly increased in HFS vs. CTRL (p<0.05; 90.4 ± 6.3 vs. 73.4 ± 4.7 nmol/g).

Myocardial CK and LDH activities as markers of cellular integrity were similar in CTRL (11.03 ± 0.44 and 3.97 ± 0.28 U/mg protein) and HFS (10.65 ± 0.55 and 3.97 ± 0.25 U/mg protein) groups after ischemia-reperfusion injury. In both groups, the active form of caspase-3 protein, was not expressed in hearts (data not shown) suggesting absence of apoptosis.

<u>**3.4 Correlation analyses**</u>

Correlation analyses are shown in Figure 6. FFAs, intrahepatic TG and percentage of functional recovery during reperfusion were correlated with the amount of VAT measured by MRI (respectively r²=0.68; r²=0.88 and r²=0.46).

4. <u>Discussion</u>

The aim of this study was to investigate the effects of long-term high-fat high-sucrose diet-feeding i) on the development of prediabetes and/or metabolic syndrome (MetS), ii) on cardiac parameters and iii) on myocardial tolerance to ischemia-reperfusion injury in female Wistar rats. Here, the emergence of a prediabetic state combined with metabolic disturbances has led to cardiac remodeling characterized by thickening of the myocardial wall, and to

increased myocardial perfusion. High-fat high-sucrose diet also decreased the sensitivity of the heart to ischemia-reperfusion injury characterized by an impairment of cardiac function, energy metabolism and endothelial function. Finally, biochemical analyses in heart tissue highlighted eNOS uncoupling, decreased S-Glutathionylation of proteins and increased MDA in HFS compared with CTRL, indicating exacerbated oxidative stress.

Diet-induced models appear to be one of the best strategies to study prediabetic and MetS conditions associated with CV complications. In 2016, Wong et al. reviewed the different existing types of diet [27]. To get closer to human disease, Panchal et al. suggested to use a combination of fat- and carbohydrate-enriched diet, which groups a maximum of criteria and leads to cardiac dysfunction and hypertrophy in rats after 16 weeks of diet [28]. Here we used high-fat high-sucrose diet containing 19.4% of protein, 35.8% of fat and 32.1% of carbohydrate. After five months of diet, animals displayed the typical characteristics for diagnosis of prediabetes (higher fasting glucose and lower glucose tolerance), which were associated with metabolic disturbances that could lead to MetS and type 2 diabetes. While many studies [29] showed increased body weight in animals under various high-fat diets, we found that the weight of female HFS rats was not significantly increased in comparison with the control group. Aubin et al. reported the same observation in their study on female Sprague Dawley rats fed with HFD for 8 weeks [30]. Nishikawa et al. suggested that the female sex could be more resistant to high-fat diet-induced obesity, which could explain our results [31]. Also, food intake was lower in HFS rats, possibly because the high-fat high-sucrose diet was more caloric. Consistent with this explanation, an increase of serum leptin, the hormone regulating satiety, has been previously reported in rats under high-fat diet [32]. Despite a possible regulatory mechanism via leptin, HFS animals had a higher caloric intake leading to abdominal obesity. Indeed, HFS rats did not display weight gain but MRI and dissection highlighted an abdominal obesity with significant increase of fat mass percentage (of both VAT and SCAT). Multiple human studies have shown that waist circumference, an indicator of abdominal obesity, is more representative of total body fat than BMI [33]. Interestingly, the amount of VAT was correlated with changes in plasma FFAs and hepatic TG content. Moreover, VAT was also correlated to the percentage of functional recovery after ischemia-reperfusion injury. These observations confirm that the anatomical distribution of excess fat is closely related to the occurrence of cardiovascular and metabolic complications [34], even in subject with normal weight [35]. Expansion and dysfunction of visceral adipose tissue both result in the release of fatty acids into the circulation and in ectopic fat deposition in organs

like heart, liver or pancreas [36]. Here, we found an increase in plasma free fatty acids and LDL-cholesterol associated with an increase in intrahepatic TG content. The increase in myocardial TG content seems to occur later than the increase of hepatic TG content, as shown in male mice under high-fat high-sucrose diet [17]. This may explain why we found no difference between groups regarding cardiac TG content in this study. Finally, in this model we would expect an increase in arterial blood pressure, as described by Aubin et al. in female high-fat fed rats [30]. Here, only a non-significant tendency to elevated systolic and diastolic blood pressures was observed in the HFS group, warranting further investigation on a larger animal group.

The combination of these risk factors predisposes women to CV complications. As shown by Levitzky et al. the risk of CV disease at lower glucose levels is higher in women than in men [7]. However, the mechanisms involved are not yet fully understood, and literature studies on female sex are scarce. Here, we followed female rats over months using cardiac MRI and observed multiple cardiac abnormalities. First, cardiac morphology was modified starting at the third month of diet with an increased myocardial wall thickness in systole and diastole. Left ventricular mass evaluated by MRI was increased at three and four months of high-fat high-sucrose diet. Concentric remodeling may occur, for example, as a result of pressure overload (such as high blood pressure or aortic stenosis) whether or not there is ventricular hypertrophy (defined as an increase in mass) [37]. Cardiomyocyte hypertrophy and cardiac fibrosis [37] could also explain the cardiac remodeling found here. However, we note that heart weight to tibia length ratio obtained *ex vivo* was not significantly higher in HFS compared to CTRL. We attribute this apparent inconsistency to the difference in methodology of measurement *in vivo* and *ex vivo*. MRI evaluation of hypertrophy was based on an ellipsoid model [14] evaluating the left ventricle only. *Ex vivo*, we measured the weight of the entire heart just before cannulation, i.e. without potential biases by blood pressure and circulation. Dedicated histology experiments may help confirm this result in future studies.

Left-ventricular cardiac function parameters evaluated by MRI were not different in female rats submitted to high-fat high-sucrose diet for 5 months compared with CTRL, whereas *ex vivo* basal cardiac function was significantly weaker. The *in vivo* cardiac function measurements reflect dynamic volume measurements whereas *ex vivo* function reflects pressure developed during contraction. Also, *ex vivo* cardiac function is not submitted to the effective regulations and demands *in vivo*. A similar difference between *in vivo* and *ex vivo* cardiac function was found by Cole et al., who found normal cardiac function *in vivo* in rats

submitted to high-fat diet but 21% decreased cardiac efficiency *ex vivo* compared with controls [38]. They related the lower cardiac efficiency to an increase in myocardial oxygen consumption. In our study, along with cardiac function we monitored myocardial perfusion *in vivo*, which may be linked to oxygen consumption. Interestingly, myocardial perfusion was significantly higher in HFS vs. CTRL, despite normal *in vivo* cardiac function, consistent with the study by Cole et al. We thus hypothesized that HFS hearts needed higher capillary blood flow to produce the same work indicating decreased cardiac efficiency. Moreover, increased myocardial perfusion might be a transient condition found in prediabetic animals [39]. In fact, a previous study in our laboratory showed decreased myocardial perfusion in type 2 diabetic male mice under high-fat high-sucrose diet [17]. Also, Iltis et al. showed defective myocardial blood flow in 8-13 months type 2 diabetic GK rats [40]. Then, it would be interesting to test this diet over a longer period to evaluate whether myocardial perfusion decreases below normal values at later stages in this model as well. Another study in type 1 diabetic patients reported higher myocardial perfusion at rest than in healthy controls [41]. Finally, it is well known that myocardial perfusion can be modified by isoflurane concentration, temperature or heart rate, and that perfusion values likely reflect partial vasodilation [42]. However, these parameters were monitored during the MRI exam and were not different between the groups (data not shown).

In summary, 5 months of high-fat high-sucrose diet induced modification of cardiac morphology and efficiency. Using the ischemia-reperfusion *ex vivo* protocol, we further found higher sensitivity to ischemia-reperfusion injury in HFS compared with CTRL, characterized by a significant decrease in myocardial function and energy metabolism during reperfusion. Under physiological conditions mitochondria play a fundamental role in oxidative catabolism leading to the production of energy in the form of ATP. Multiple mitochondrial impairments could be responsible for lower energy metabolism. Among these are mitochondrial uncoupling [38], decreased expression of mitochondrial respiratory chain complex or increased ROS production. Moreover, a loss of nucleotide precursors limiting ATP repletion during reperfusion could contribute to our observation. Because these alterations may be correlated with oxidative stress, we particularly focused on myocardial MDA content as lipid peroxidation marker, which was significantly higher in HFS vs. CTRL. Pakdeechote et al. have previously reported higher vascular superoxide production as well as higher MDA levels in plasma in metabolic syndrome rats [43]. Poudyal et al. also showed lowered capacity to neutralize free radicals characterized by the decrease of antioxidant capacity [29]. Finally,

ischemia and mostly reflow are well-known to induce high oxidative stress, which is exacerbated here by the 5-month high-fat high-sucrose diet. We also assessed the S-Glutathionylation of proteins, which is the reversible addition of glutathione to cysteine residues inactivating the target proteins [44], and which could be involved in CV complications [45]. Protein S-Glutathionylation occurs mainly at the beginning of reflow in an ischemia-reperfusion protocol and has been shown to be increased in some studies. For example, De Pascali et al. showed an increase in eNOS S-Glutathionylation during ischemia-reperfusion injury in endothelial cells [46]. However, Belcastro et al. explained that S-Glutathionylation can also be a protective mechanism coping with irreversible oxidation [45]. This would explain the lower rate of S-Glutathionylation found here in HFS vs. CTRL. We have shown that S-Glutathionylation of all the proteins was significantly decreased in HFS compared with CTRL, but we found no difference in specific S-Glutathionylation of eNOS. Here, we suggest that S-Glutathionylation was decreased by high-fat high-sucrose diet, leading to higher level of damage by oxidative stress in hearts. This result was consistent with the higher MDA heart content mentioned before.

Prediabetes and MetS increase the risk of cardiovascular events and have a deleterious impact on endothelial function with enhanced coronary artery disease prevalence [47]. Altered vasodilatation has been previously described. Poudyal et al. showed lower vascular response to noradrenaline, acetylcholine and sodium nitroprusside in a MetS model [29] while Senaphan et al. found decreased eNOS expression in mesenteric arteries [48]. Here, no significant difference was found in coronary flow before ischemia. During reperfusion, however, coronary flow was significantly impaired in HFS vs. CTRL, indicating higher sensitivity of coronary arteries to ischemia-reperfusion injury. We found no difference between the groups concerning the expression of total eNOS or its phosphorylated form. However, we found higher eNOS uncoupling in HFS compared with CTRL, with a lower dimeric (active) form of eNOS and a higher monomer form of eNOS in hearts, indicating that high-fat high-sucrose diet impaired eNOS activity. eNOS uncoupling is known to be responsible for the increase in superoxide anion $O_2^{\cdot-}$ production instead of NO [49]. $O_2^{\cdot-}$ is highly deleterious for the cells and can also react with NO to form peroxynitrite ($ONOO^-$), making it less available for endothelial function. $ONOO^-$ has been shown to inhibit mitochondrial respiratory chain complex [50]. During reperfusion this phenomenon is amplified because the free electrons couple to oxygen to form $O_2^{\cdot-}$. Moreover, patients with MetS show lower levels of superoxide dismutase able to handle superoxide anion [51].

Endothelial function also seems to be a key point in cardiac complications of type 2 diabetes. Desrois et al. showed endothelial impairment in female Goto-Kakizaki rats, with lower coronary flow and reduced up-regulation of the NO pathway [22]. Zhang et al. revealed a predisposition of females to vascular lesions after induction of diabetes, in the mesenteric arteries [52] and the aorta [53]. Thus, endothelial dysfunction found in our model of prediabetes could be related to the higher cardiovascular risk in prediabetic and type 2 diabetic women.

As a perspective, it would be interesting to measure plasma hormones in order to fully elucidate their role in high-fat high-sucrose diet-induced cardiovascular modifications. Baseline cardiac function differs between sexes in terms of heart rate, systolic output, ejection fraction [54]. Studies on rodents [55] have shown that cardiac myocytes of male rats contract stronger and faster than the myocytes of female rats. Estrogen receptors (ERα and β) are both found in cardiomyocytes and may have a strong impact on cardiovascular function [56]. Estrogens have been shown to protect the heart from ischemic injury [57]. The loss of estrogens also leads to aggravation of mitochondrial dysfunction, inflammation and cardiac remodeling [58]. Sex hormones could also explain the differences found in endothelial function, as reported by Khalil et al., who showed that estrogen might directly stimulate NO production in women [59]. Interestingly, Al-Mulla et al reported a decrease in estrogens and an increase in testosterone levels in the GK rat model [60]. However, in a model of high-fat diet, Chakraborty et al. reported an increase in estradiol level with high-fat diet [61]. In addition, assessing the cytokine profiles in HFS rats could help us understand diet-induced metabolic and structural changes that occur before ischemia-reperfusion injury. Indeed, Pakdeechote et al. reported higher plasma TNFα and increased expression of iNOS in aorta of rat with diet-induced metabolic syndrome [43]. In future studies it would also be interesting to have dedicated groups for histology investigations. Previous studies showed that 16 weeks of high-carbohydrate high-fat diet could induce cardiomyocyte hypertrophy, as well as left ventricular interstitial collagen deposition and inflammatory cell infiltration in rat hearts [29, 37, 62]. Finally, dietary interventions could prevent cardiac changes observed in prediabetic female rats. Abdurrachim et al. showed that intermittent fasting could delay the progression of left ventricular hypertrophy and prevent cardiac dysfunction in prediabetic obese spontaneous hypertensive heart failure rats, by modulating cardiac substrate metabolism [63]. Alam et al. showed for example that chronic L-Arginine treatment improved metabolic, cardiovascular and liver complications in diet-induced obesity in rats [62]. We also believe

that an antioxidant approach would be of great interest in our context. For example, Resveratrol, a polyphenol, well-known for its anti-oxidant property, can protect the heart of high-fat fed rats [64].

5. Limitation of the study

One limitation of our study might be the absence of male groups, which could help us demonstrate sex-specific response to high-fat high-sucrose diet on cardiovascular alterations. However, we believe this is an original study on female sex which is little explored in the literature. Indeed, most of the studies use male population only, although type 2 diabetic women have a higher cardiovascular risk than type 2 diabetic men. Here, our objective was to study the female population by performing a longitudinal follow-up at the beginning of the disease and to observe the early adaptation of the heart to prediabetes. It brings new insights on cardiovascular complications in female rats during the development of prediabetes, with increased myocardial perfusion as well as high sensitivity to ischemia-reperfusion injury via impaired energy metabolism, S-Glutathionylation and eNOS uncoupling.

6. Conclusion

To our knowledge, this is the first study combining a longitudinal cardiac MRI follow-up with an assessment of tolerance to ischemic insult in prediabetic female rats under high-fat high-sucrose diet. In female rats, prediabetes led to myocardial adaptation over months characterized by thickening of the myocardial wall and increase in myocardial perfusion. It also led to higher cardiac sensitivity to ischemia-reperfusion injury. Oxidative stress seems to be at the intersection of the pathways elucidated here, as shown in Figure 7. Oxidative stress, induced by ischemia-reperfusion, was exacerbated under high-fat high-sucrose diet. Here, it might be responsible for i) cardiac dysfunction via impaired energy metabolism with altered ATP and PCr production during ischemia-reperfusion injury, ii) endothelial dysfunction via eNOS uncoupling and decreased NO bioavailability leading to lower coronary flow, and iii) decrease of protective protein S-Glutathionylation mechanism. This work provides insights that may contribute to understanding the cardiovascular complications related to prediabetes and type 2 diabetes in the female sex.

Declarations

List of abbreviations

CF: Coronary Flow, CK: Creatine Kinase, CV: Cardiovascular, DP: Developed Pressure, eNOS: Endothelial NO Synthase, P-eNOS: Phosphorylated form of eNOS, HR: Heart Rate, LDH: Lactate Dehydrogenase, MDA: Malondialdehyde, MetS: Metabolic Syndrome, MRS: Magnetic Resonance Spectroscopy, NO: Nitric Oxide, ONOO$^-$: Peroxynitrite, SCAT: Subcutaneous Adipose Tissue, TG: Triglycerides, VAT: Visceral Adipose Tissue.

References

[1]   Cho NH, Shaw JE, Karuranga S, Huang Y, da Rocha Fernandes JD, Ohlrogge AW, et al. IDF Diabetes Atlas: Global estimates of diabetes prevalence for 2017 and projections for 2045. Diabetes Res Clin Pract 2018;138:271-81. 10.1016/j.diabres.2018.02.023.

[2]   Huxley R, Barzi F and Woodward M. Excess risk of fatal coronary heart disease associated with diabetes in men and women: meta-analysis of 37 prospective cohort studies. BMJ : British Medical Journal 2006;332:73-8. 10.1136/bmj.38678.389583.7C.

[3]   Wannamethee S, Papacosta O, Lawlor D, Whincup P, Lowe G, Ebrahim S, et al. Do women exhibit greater differences in established and novel risk factors between

diabetes and non-diabetes than men? The British Regional Heart Study and British Women's Heart Health Study. Diabetologia 2012;55:80-7.

[4]   Grundy SM. Pre-diabetes, metabolic syndrome, and cardiovascular risk. J Am Coll Cardiol 2012;59:635-43. 10.1016/j.jacc.2011.08.080.

[5]   Veugen M, Onete V, Koster A, Dagnelie P, Schaper N, van der Kallen C, et al. 54(th) EASD Annual Meeting of the European Association for the Study of Diabetes : Berlin, Germany, 1 - 5 October 2018. Diabetologia 2018;61:1-620. 10.1007/s00125-018-4693-0.

[6]   Donahue RP, Dorn JM, Stranges S, Swanson M, Hovey K and Trevisan M. Impaired fasting glucose and recurrent cardiovascular disease among survivors of a first acute myocardial infarction: evidence of a sex difference? The Western New York experience. Nutrition, metabolism, and cardiovascular diseases: NMCD 2011;21:504-11. 10.1016/j.numecd.2009.11.012.

[7]   Levitzky Y, Pencina M, D'Agostino R, Meigs J, Murabito J, Vasan R, et al. Impact of impaired fasting glucose on cardiovascular disease: the Framingham Heart Study. J Am Coll Cardiol 2008;51:264-70.

[8]   Huang D, Refaat M, Mohammedi K, Jayyousi A, Al Suwaidi J and Abi Khalil C. Macrovascular Complications in Patients with Diabetes and Prediabetes. Biomed Res Int 2017;2017:7839101. 10.1155/2017/7839101.

[9]   Alberti K, Eckel R, Grundy S, Zimmet P, Cleeman J, Donato K, et al. Harmonizing the Metabolic Syndrome: A Joint Interim Statement of the International Diabetes Federation Task Force on Epidemiology and Prevention; National Heart, Lung, and Blood Institute; American Heart Association; World Heart Federation; International Atherosclerosis Society; and International Association for the Study of Obesity. Circulation 2008;120:1640-5.

[10]   Ford E. Risks for all-cause mortality, cardiovascular disease, and diabetes associated with the metabolic syndrome: a summary of the evidence. . Diabetes Care 2005;28:1769-78.

[11]   Hu G, Qiao Q, Tuomilehto J, Balkau B, Borch-Johnsen K, Pyorala K, et al. Prevalence of the metabolic syndrome and its relation to all-cause and cardiovascular mortality in nondiabetic European men and women. - PubMed - NCBI. Archives of Internal Medicine 2004;164:1066-76.

[12]   Mainous AG, 3rd, Tanner RJ, Jo A and Anton SD. Prevalence of Prediabetes and Abdominal Obesity Among Healthy-Weight Adults: 18-Year Trend. Ann Fam Med 2016;14:304-10. 10.1370/afm.1946.

[13]   Wagner A, Dallongeville J, Haas B, Ruidavets JB, Amouyel P, Ferrières J, et al. Sedentary behaviour, physical activity and dietary patterns are independently associated with the metabolic syndrome. Diabetes & Metabolism 2012;38:428-35. 10.1016/j.diabet.2012.04.005.

[14]   Kober F, Iltis I, Cozzone P and Bernard M. Cine-MRI assessment of cardiac function in mice anesthetized with ketamine/xylazine and isoflurane. MAGMA 2004;17:157-61. 10.1007/s10334-004-0086-0.

[15]   Kober F, Iltis I, Izquierdo M, Desrois M, Ibarrola D, Cozzone P, et al. High-resolution myocardial perfusion mapping in small animals in vivo by spin-labeling gradient-echo imaging. Magnetic Resonance in Medicine 2004;51:62-7. 10.1002/mrm.10676.

[16]   Gaborit B, Kober F, Jacquier A, Moro PJ, Cuisset T, Boullu S, et al. Assessment of epicardial fat volume and myocardial triglyceride content in severely obese subjects: relationship to metabolic profile, cardiac function and visceral fat. International Journal of Obesity (2005) 2012;36:422-30. 10.1038/ijo.2011.117.

[17]   Abdesselam I, Pepino P, Troalen T, Macia M, Ancel P, Masi B, et al. Time course of cardiometabolic alterations in a high fat high sucrose diet mice model and improvement after GLP-1 analog treatment using multimodal cardiovascular magnetic resonance. Journal of Cardiovascular Magnetic Resonance: Official Journal of the Society for Cardiovascular Magnetic Resonance 2015;17:95. 10.1186/s12968-015-0198-x.

[18]   Mattei J, Fur Y, Cuge N, Guis S, Cozzone P and Bendahan D. Segmentation of fascias, fat and muscle from magnetic resonance images in humans: the DISPIMAG software. MAGMA 2006;19:275-9.

[19]   Achard V, Sanchez C, Tassistro V, Verdier M, Alessi M and Grino M. Immediate Postnatal Overfeeding in Rats Programs Aortic Wall Structure Alterations and Metalloproteinases Dysregulation in Adulthood. Am J Hypertens 2016;29:719-26.

[20]   Desrois M, Clarke K, Lan C, Dalmasso C, Cole M, Portha B, et al. Upregulation of eNOS and unchanged energy metabolism in increased susceptibility of the aging type 2 diabetic GK rat heart to ischemic injury. American Journal of Physiology. Heart and Circulatory Physiology 2010;299:H1679-86. 10.1152/ajpheart.00998.2009.

[21]   Lopaschuk G. Alterations in fatty acid oxidation during reperfusion of the heart after myocardial ischemia. The American Journal of Cardiology 1997;80:11A-6A.

[22]   Desrois M, Lan C, Movassat J and Bernard M. Reduced up-regulation of the nitric oxide pathway and impaired endothelial and smooth muscle functions in the female type 2 diabetic goto-kakizaki rat heart. Nutrition & Metabolism 2017;14:6. 10.1186/s12986-016-0157-z.

[23]   Desrois M, Sciaky M, Lan C, Cozzone PJ and Bernard M. L-arginine during long-term ischemia: effects on cardiac function, energetic metabolism and endothelial damage. The Journal of Heart and Lung Transplantation: The Official Publication of the International Society for Heart Transplantation 2000;19:367-76.

[24]   Huffman L, Koch S and Butler K. Coronary effluent from a preconditioned heart activates the JAK-STAT pathway and induces cardioprotection in a donor heart. Am J Physiol Heart Circ Physiol 2008;294:H257-62.

[25]   Farah C, Kleindienst A, Bolea G, Meyer G, Gayrard S, Geny B, et al. Exercise-induced cardioprotection: a role for eNOS uncoupling and NO metabolites. . Basic Research in Cardiology 2013;108:389.

[26]   Kleindienst A, Battault S, Belaidi E, Tanguy S, Rosselin M, Boulghobra D, et al. Exercise does not activate the β3 adrenergic receptor-eNOS pathway, but reduces inducible NOS expression to protect the heart of obese diabetic mice. Basic Research in Cardiology 2016;111:40. 10.1007/s00395-016-0559-0.

[27]   Wong SK, Chin K-Y, Suhaimi FH, Fairus A and Ima-Nirwana S. Animal models of metabolic syndrome: a review. Nutrition & Metabolism 2016;13:65. 10.1186/s12986-016-0123-9.

[28]   Panchal SK and Brown L. Rodent models for metabolic syndrome research. Journal of Biomedicine & Biotechnology 2011;2011:351982. 10.1155/2011/351982.

[29]   Poudyal H, Campbell F and Brown L. Olive leaf extract attenuates cardiac, hepatic, and metabolic changes in high carbohydrate-, high fat-fed rats. The Journal of Nutrition 2010;140:946-53. 10.3945/jn.109.117812.

[30]   Aubin MC, Lajoie C, Clement R, Gosselin H, Calderone A and Perrault LP. Female rats fed a high-fat diet were associated with vascular dysfunction and cardiac fibrosis in the absence of overt obesity and hyperlipidemia: therapeutic potential of resveratrol. J Pharmacol Exp Ther 2008;325:961-8. 10.1124/jpet.107.135061.

[31] Nishikawa S, Yasoshima A, Doi K, Nakayama H and Uetsuka K. Involvement of sex, strain and age factors in high fat diet-induced obesity in C57BL/6J and BALB/cA mice. Exp Anim 2007;56:263-72.

[32] Balasubramanian P, Jagannathan L, Mahaley RE, Subramanian M, Gilbreath ET, Mohankumar PS, et al. High fat diet affects reproductive functions in female diet-induced obese and dietary resistant rats. J Neuroendocrinol 2012;24:748-55. 10.1111/j.1365-2826.2011.02276.x.

[33] Wilner B, Garg S, Ayers CR, Maroules CD, McColl R, Matulevicius SA, et al. Dynamic Relation of Changes in Weight and Indices of Fat Distribution With Cardiac Structure and Function: The Dallas Heart Study. J Am Heart Assoc 2017;6. 10.1161/jaha.117.005897.

[34] Mantatzis M, Milousis T, Katergari S, Delistamatis A, Papachristou DN and Prassopoulos P. Abdominal adipose tissue distribution on MRI and diabetes. Academic Radiology 2014;21:667-74. 10.1016/j.acra.2014.01.009.

[35] De Larochellière E, Côté J, Gilbert G, Bibeau K, Ross M, Dion-Roy V, et al. Visceral/epicardial adiposity in nonobese and apparently healthy young adults: association with the cardiometabolic profile. Atherosclerosis 2014;234:23-9.

[36] Després J-P, Lemieux I, Bergeron J, Pibarot P, Mathieu P, Larose E, et al. Abdominal obesity and the metabolic syndrome: contribution to global cardiometabolic risk. Arteriosclerosis, Thrombosis, and Vascular Biology 2008;28:1039-49. 10.1161/ATVBAHA.107.159228.

[37] Panchal SK, Poudyal H, Iyer A, Nazer R, Alam MA, Diwan V, et al. High-carbohydrate, high-fat diet-induced metabolic syndrome and cardiovascular remodeling in rats. Journal of Cardiovascular Pharmacology 2011;57:611-24. 10.1097/FJC.0b013e31821b1379.

[38] Cole MA, Murray AJ, Cochlin LE, Heather LC, McAleese S, Knight NS, et al. A high fat diet increases mitochondrial fatty acid oxidation and uncoupling to decrease efficiency in rat heart. Basic Research in Cardiology 2011;106:447-57. 10.1007/s00395-011-0156-1.

[39] Nagarajan V, Kohan L, Holland E, Keeley EC and Mazimba S. Obesity paradox in heart failure: a heavy matter. ESC Heart Failure 2016;3:227-34. 10.1002/ehf2.12120.

[40] Iltis I, Kober F, Desrois M, Dalmasso C, Lan C, Portha B, et al. Defective myocardial blood flow and altered function of the left ventricle in type 2 diabetic rats: a noninvasive in vivo study using perfusion and cine magnetic resonance imaging. Investigative Radiology 2005;40:19-26.

[41] Byrne C, Jensen T, Hjortkjaer HO, Mogensen UM, Kuhl JT, Fuchs A, et al. Myocardial perfusion at rest in patients with Diabetes Mellitus Type 1 compared with healthy controls assessed with Multi Detector Computed Tomography. Diabetes Res Clin Pract 2015;107:15-22. 10.1016/j.diabres.2014.10.011.

[42] Iltis I, Kober F, Dalmasso C, Lan C, Cozzone PJ and Bernard M. In vivo assessment of myocardial blood flow in rat heart using magnetic resonance imaging: effect of anesthesia. Journal of magnetic resonance imaging: JMRI 2005;22:242-7. 10.1002/jmri.20352.

[43] Pakdeechote P, Bunbupha S, Kukongviriyapan U, Prachaney P, Khrisanapant W and Kukongviriyapan V. Asiatic acid alleviates hemodynamic and metabolic alterations via restoring eNOS/iNOS expression, oxidative stress, and inflammation in diet-induced metabolic syndrome rats. Nutrients 2014;6:355-70. 10.3390/nu6010355.

[44] Belcastro E, Gaucher C, Corti A, Leroy P, Lartaud I and Pompella A. Regulation of protein function by S-nitrosation and S-glutathionylation: processes and targets in

cardiovascular pathophysiology. Biological Chemistry 2017;398:1267-93. 10.1515/hsz-2017-0150.

[45]   Goel A, Thor D, Anderson L and Rahimian R. Sexual dimorphism in rabbit aortic endothelial function under acute hyperglycemic conditions and gender-specific responses to acute 17beta-estradiol. American Journal of Physiology. Heart and Circulatory Physiology 2008;294:H2411-20. 10.1152/ajpheart.01217.2007.

[46]   De Pascali F, Hemann C, Samons K, Chen C-A and Zweier JL. Hypoxia and reoxygenation induce endothelial nitric oxide synthase uncoupling in endothelial cells through tetrahydrobiopterin depletion and S-glutathionylation. Biochemistry 2014;53:3679-88. 10.1021/bi500076r.

[47]   Wilson PW, Kannel WB, Silbershatz H and D'Agostino RB. Clustering of metabolic factors and coronary heart disease. Archives of Internal Medicine 1999;159:1104-9.

[48]   Senaphan K, Kukongviriyapan U, Sangartit W, Pakdeechote P, Pannangpetch P, Prachaney P, et al. Ferulic Acid Alleviates Changes in a Rat Model of Metabolic Syndrome Induced by High-Carbohydrate, High-Fat Diet. Nutrients 2015;7:6446-64. 10.3390/nu7085283.

[49]   Forstermann U and Sessa WC. Nitric oxide synthases: regulation and function. Eur Heart J 2012;33:829-37, 37a-37d. 10.1093/eurheartj/ehr304.

[50]   Brown GC and Borutaite V. Nitric oxide and mitochondrial respiration in the heart. Cardiovasc Res 2007;75:283-90. 10.1016/j.cardiores.2007.03.022.

[51]   Sabir AA, Bilbis LS, Saidu Y, Jimoh A, Iwuala SO, Isezuo SA, et al. Oxidative stress among subjects with metabolic syndrome in Sokoto, North-Western Nigeria. Nigerian Journal of Clinical Practice 2016;19:128-32. 10.4103/1119-3077.173705.

[52]   Zhang R, Thor D, Han X, Anderson L and Rahimian R. Sex differences in mesenteric endothelial function of streptozotocin-induced diabetic rats: a shift in the relative importance of EDRFs. American Journal of Physiology. Heart and Circulatory Physiology 2012;303:H1183-98. 10.1152/ajpheart.00327.2012.

[53]   Han X, Zhang R, Anderson L and Rahimian R. Sexual dimorphism in rat aortic endothelial function of streptozotocin-induced diabetes: possible involvement of superoxide and nitric oxide production. European Journal of Pharmacology 2014;723:442-50. 10.1016/j.ejphar.2013.10.052.

[54]   Parks RJ and Howlett SE. Sex differences in mechanisms of cardiac excitation-contraction coupling. Pflugers Arch 2013;465:747-63. 10.1007/s00424-013-1233-0.

[55]   Blenck CL, Harvey PA, Reckelhoff JF and Leinwand LA. The Importance of Biological Sex and Estrogen in Rodent Models of Cardiovascular Health and Disease. Circ Res 2016;118:1294-312. 10.1161/circresaha.116.307509.

[56]   Murphy E. Estrogen signaling and cardiovascular disease. Circ Res 2011;109:687-96. 10.1161/circresaha.110.236687.

[57]   Knowlton AA and Korzick DH. Estrogen and the female heart. Mol Cell Endocrinol 2014;389:31-9. 10.1016/j.mce.2014.01.002.

[58]   Li S and Gupte AA. The Role of Estrogen in Cardiac Metabolism and Diastolic Function. Methodist Debakey Cardiovasc J 2017;13:4-8. 10.14797/mdcj-13-1-4.

[59]   Khalil RA. Sex hormones as potential modulators of vascular function in hypertension. Hypertension 2005;46:249-54. 10.1161/01.HYP.0000172945.06681.a4.

[60]   Al-Mulla F, Leibovich SJ, Francis IM and Bitar MS. Impaired TGF-beta signaling and a defect in resolution of inflammation contribute to delayed wound healing in a female rat model of type 2 diabetes. Mol Biosyst 2011;7:3006-20. 10.1039/c0mb00317d.

[61]   Chakraborty TR, Donthireddy L, Adhikary D and Chakraborty S. Long-Term High Fat Diet Has a Profound Effect on Body Weight, Hormone Levels, and Estrous Cycle in Mice. Med Sci Monit 2016;22:1601-8.

[62] Alam MA, Kauter K, Withers K, Sernia C and Brown L. Chronic l-arginine treatment improves metabolic, cardiovascular and liver complications in diet-induced obesity in rats. Food & Function 2013;4:83-91. 10.1039/c2fo30096f.

[63] Abdurrachim D, Teo XQ, Woo C-C, Lalic J and Lee P. 54(th) EASD Annual Meeting of the European Association for the Study of Diabetes : Berlin, Germany, 1 - 5 October 2018. Diabetologia 2018;61:1-620. 10.1007/s00125-018-4693-0.

[64] Meng C, Liu JL and Du AL. Cardioprotective effect of resveratrol on atherogenic diet-fed rats. Int J Clin Exp Pathol 2014;7:7899-906.

Compounds	%
Casein	22.8
DL methionine	0.2
Maltodextrin	17.15
Sucrose	16.64
Anhydrous butter	33.35
Soya oil	2.5
Mineral (AIN 93G-mx)	4.55
Sodium bicarbonate	1.05
Potassium citrate	0.4
Vitamin (AIN 93-vx)	1.3
Choline bitartrate	0.2
Antioxidant	0.002

**Table 1: Composition of the high-fat high-sucrose diet (SAFE, U8978).**

	CTRL	HFS	note
Body weight (g)	270.1 ± 11.2	297.8 ± 17.3	
Lean mass (g)	262.8 ± 7.4	271.7 ± 9.1	
Food intake for 5 months (g)	1514 ± 26	1031 ± 10.8 *	
Calories intake for 5 months (kcal)	5054 ± 87	5669 ± 59 *	
AUC Food efficiency (weight gain/food intake)	0.31 ± 0.04	0.50 ± 0.05 †	
Systolic blood pressure (mm Hg)	111.7 ± 3.3	128.7 ± 10.4	
Diastolic blood pressure (mm Hg)	76.1 ± 2.9	90.1 ± 8.1	
VAT MRI (volume mm^3/slice)	700 ± 63	1122 ±128 ‡	Correlation
VAT Dissection (g)	19.3 ± 3.1	38.4 ± 6.7 ‡	r²=0.90
SCAT MRI (volume mm^3/slice)	233 ± 13	402 ± 52 †	Correlation
SCAT Dissection (g)	9.89 ± 1.5	18.9 ± 4.3	r²=0.98
Cardiac TG (%)	0.28 ± 0.28	0.14 ± 0.14	
Fat mass (%)	9.8 ± 1.2	16.8 ± 2.1 ‡	
Hepatic TG (%)	0.88 ± 0.28	6.10 ± 1.27 *	
Heart weight (g)	0.76 ± 0.02	0.78 ± 0.02	
Tibia length (cm)	3.50 ± 0.04	3.48 ±0.04	
Heart weight / Tibia length (g/cm)	0.220 ± 0.005	0.230 ± 0.006	
FFAs (mM)	0.09 ± 0.01	0.21 ± 0.04 *	
Fasting glucose (mM)	4.78 ± 0.22	5.72 ± 0.17 †	
TG (mM)	125.2 ± 14.4	90.5 ± 15.2	
HDL-Cholesterol (mM)	1.24 ± 0.07	1.24 ± 0.13	
LDL-Cholesterol (mM)	0.83 ± 0.10	1.19 ± 0.13 ‡	
AUC IPGTT (mM/min)	7.1 ± 0.5	10.4 ± 0.8 †	

Table 2: Physiological characteristics of rats after 5 months of diet. Data are means ± SEM, two-way ANOVA was used for statistical analysis of IPGTT and t-test was used for all the other parameters. HFS group had lower food intake, higher calorie intake, food efficiency, amount of visceral and subcutaneous adipose tissue, % of fat mass, % of hepatic TG, plasma FFAs, fasting glucose, LDL-Cholesterol and intolerance to glucose. We found no difference

between groups for body weight, systolic blood pressure, diastolic blood pressure, cardiac TG content, heart weight-to-tibia length ratio, plasma TG and HDL-Cholesterol. AUC: area under the curve. * $p<0.001$; † $p<0.01$ and ‡ $p<0.05$ vs. CTRL.
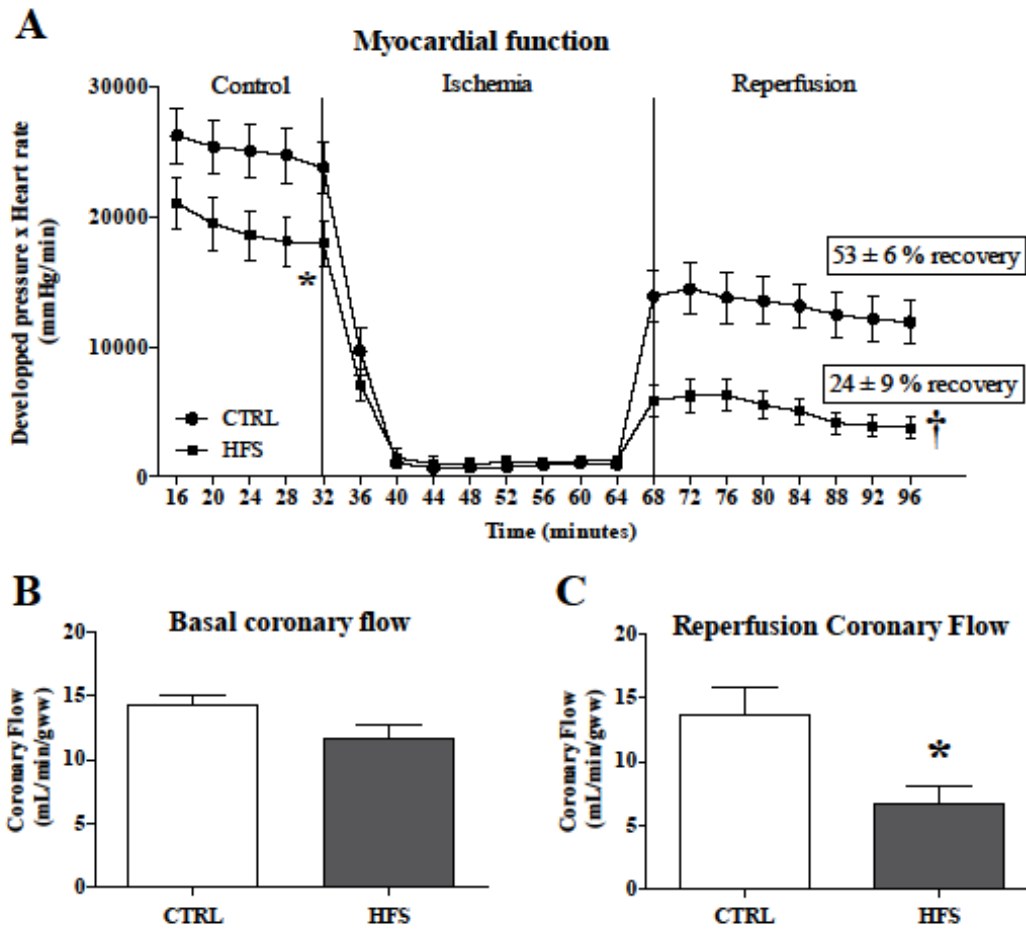
Figure 1
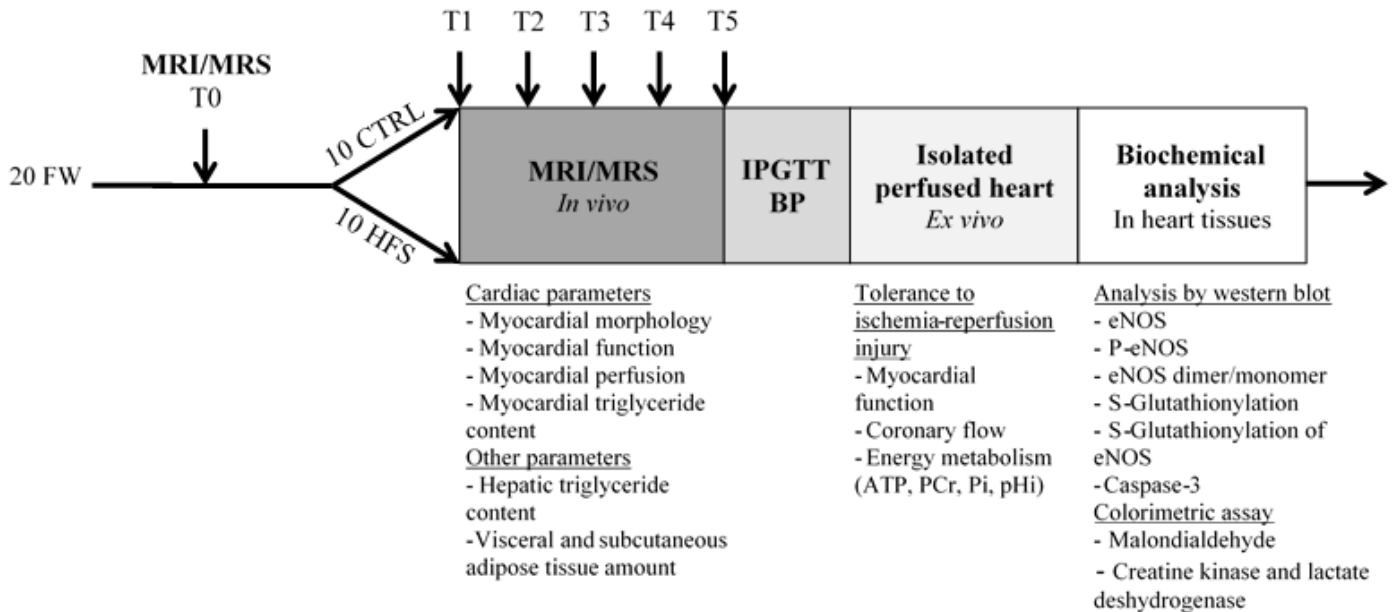
Figure 1: Experimental protocol. At 7 weeks of age, animals (n=20) underwent a first MRI/MRS investigation (T0). Female Wistar rats were randomized in two groups (CTRL and HFS), and every month an MRI/MRS exam was performed on each rat. The following parameters were evaluated: myocardial morphology, function, perfusion, triglyceride content, hepatic triglycerides and visceral and subcutaneous adipose tissue amount. After 5 months of diet, rats underwent an intraperitoneal glucose tolerance test (IPGTT) to evaluate their metabolic status, and arterial blood pressure (BP) was measured. Then, *ex vivo* experiments on isolated perfused heart were performed to evaluate tolerance to ischemia-reperfusion injury with simultaneous measurement of myocardial function, energy metabolism and coronary flow. At the end of the experiments, hearts were freeze-clamped for biochemical analysis. Western blots were performed to analyze expression of eNOS, P-eNOS, eNOS dimer/monomer, S-Glutathionylation, eNOS S-Glutathionylation and Caspase-3 proteins. Colorimetric assays were performed to assess MDA heart content and activity of creatine kinase and lactate dehydrogenase enzymes.
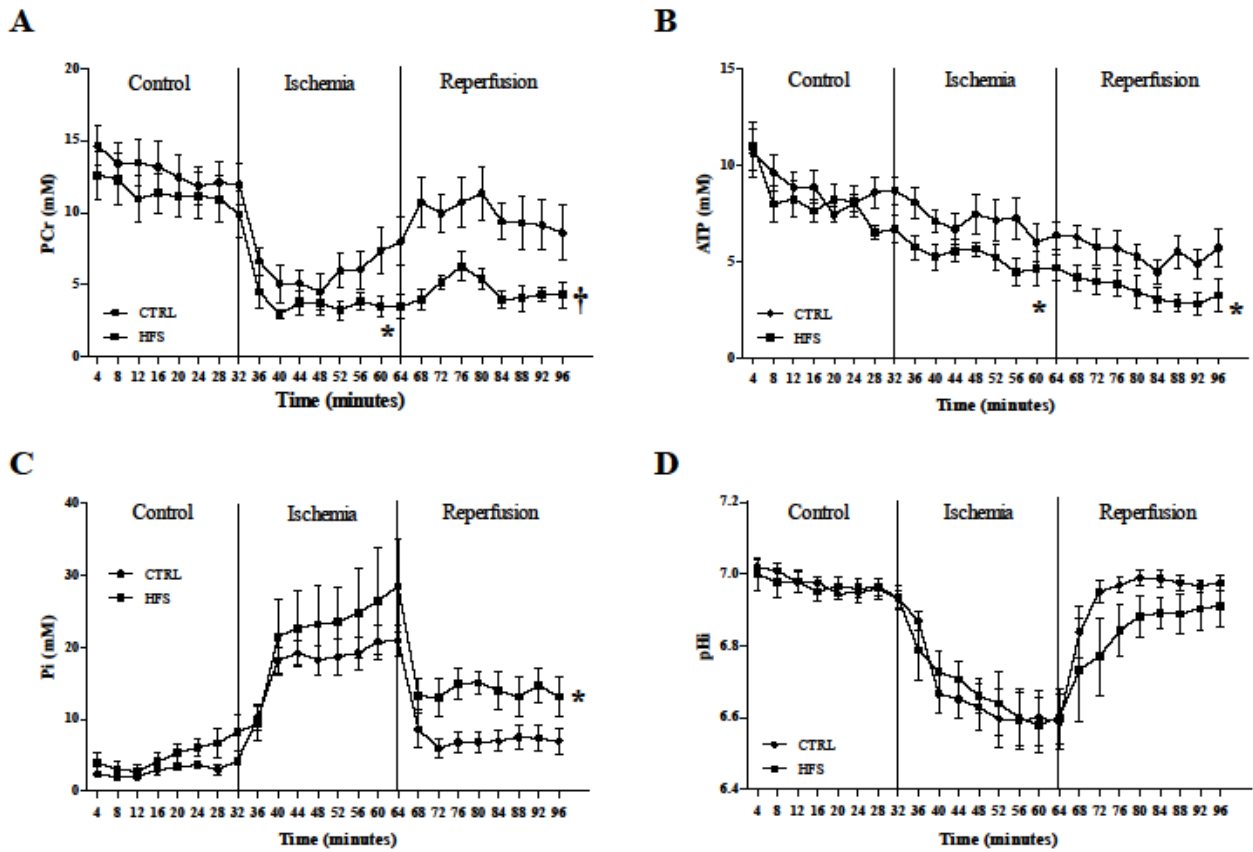
Figure 2
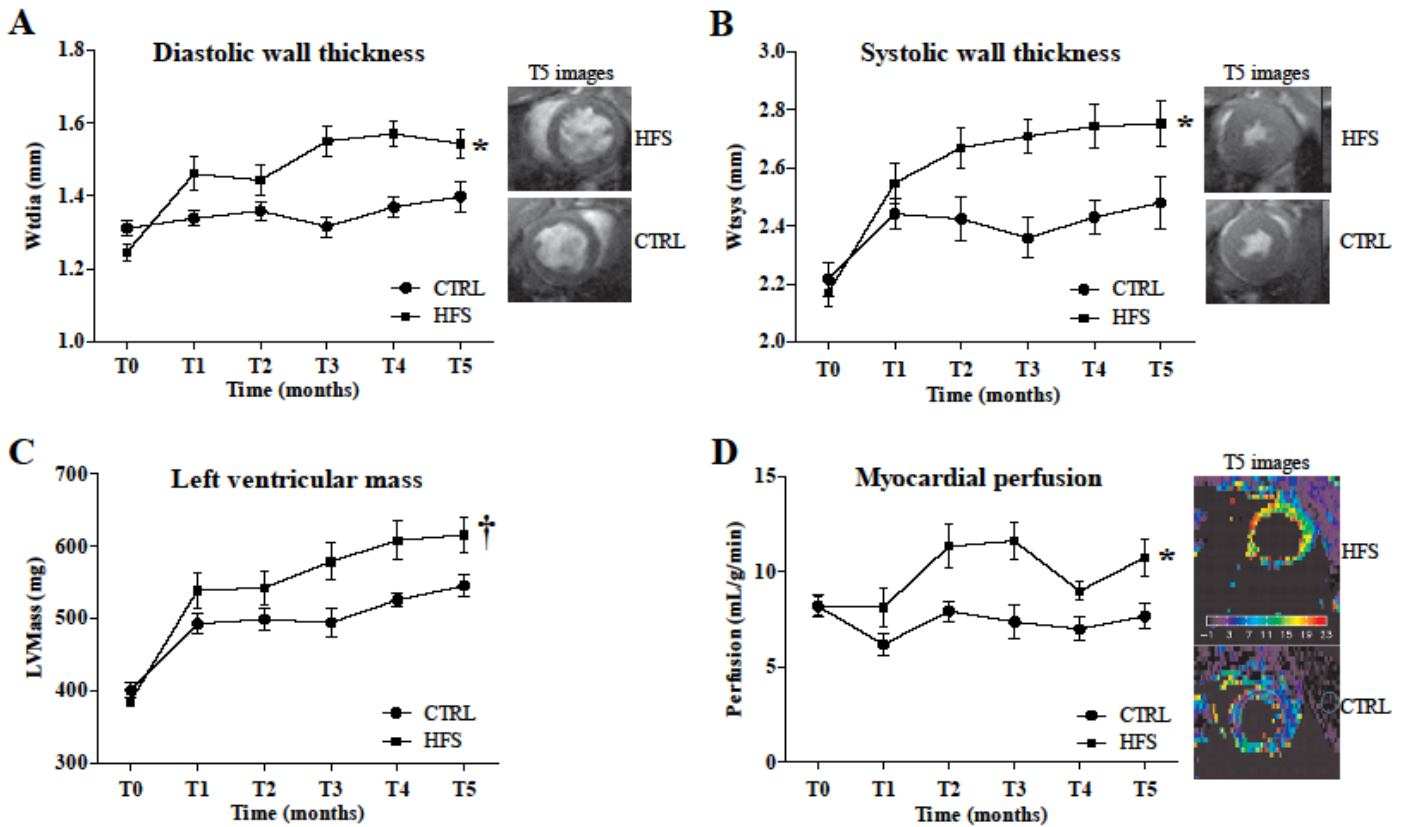
Figure 2: Monitoring of cardiac morphology and perfusion over time by MRI. Diastolic myocardial wall thickness (Wtdia) (A), Systolic myocardial wall thickness (Wtsys) (B), Left ventricular mass (LVMass) (C), Myocardial perfusion (D). Data are means ± SEM. Two-way ANOVA was performed to observe the effect of group and time. Wtdia (ANOVA: $p < 0.01$; Bonferroni post-hoc test: T3 $p < 0.001$, T4 $p < 0.001$ and T5 $p < 0.05$) and Wtsys (ANOVA: $p < 0.01$; Bonferroni post-hoc test: T3 $p < 0.01$, T4 $p < 0.01$ and T5 $p < 0.05$) were significantly increased in HFS vs. CTRL from the third month. LVMass was significantly increased in HFS at T3 and T4 months (ANOVA: $p < 0.05$; Bonferroni post-hoc test: T3 $p < 0.05$ and T4 $p < 0.01$). Myocardial perfusion was significantly increased from the second month of diet (ANOVA: $p < 0.01$; Bonferroni post-hoc test: T2 $p < 0.05$, T3 $p < 0.01$ and T5 $p < 0.05$). * $p < 0.01$ and † $p < 0.05$ vs. CTRL (Two-way ANOVA).
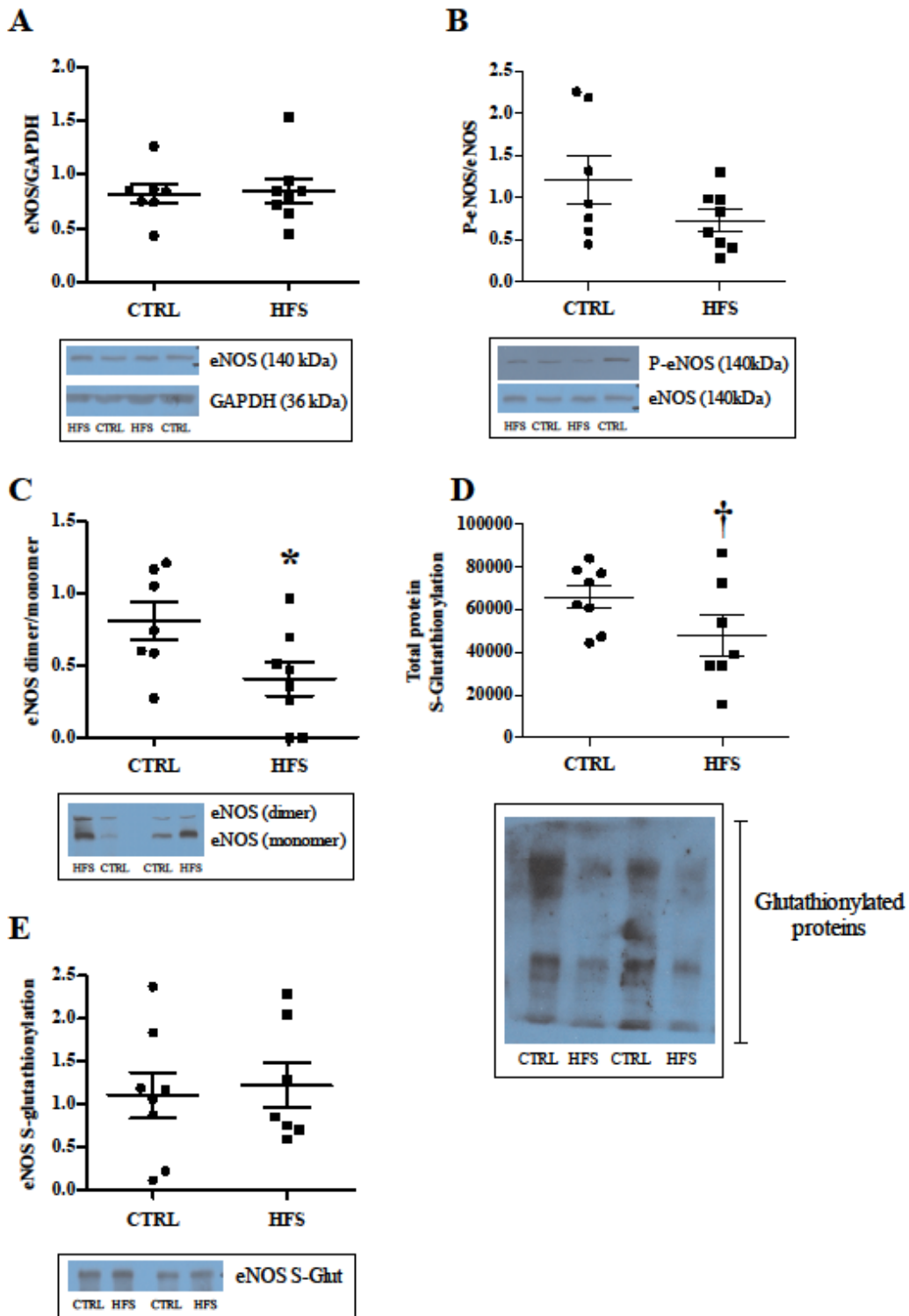
Figure 3

Figure 3: *Ex vivo* **evaluation of myocardial function.** Myocardial function (A) was evaluated by the product of developed pressure and heart rate, during the experimental time course in CTRL and HFS rat hearts. Coronary flow was measured during the control period at 20 minutes (B) and during reperfusion at 80 minutes (C) of protocol. Results are expressed as means ± SEM. For myocardial function statistical analysis, two-way ANOVA was performed to observe the effect of group and time. T-test was performed for statistical analysis of coronary flow. In HFS, myocardial function was significantly decreased during the control period and reperfusion, % of recovery and coronary flow were significantly impaired compared with CTRL. * $p < 0.05$ and † $p < 0.01$ vs. CTRL.

Figure 4

Figure 4: *Ex vivo* **evaluation of energy metabolism with** ^{31}**P-MRS.** Kinetics of phosphocreatine (PCr) (A), ATP (B), Pi (C) and intracellular pH (pHi) (D) during the experimental time course in CTRL and HFS rat hearts. Data are means ± SEM. Two-way ANOVA was performed to observe the effect of group and time. Myocardial PCr and ATP contents were significantly decreased in HFS vs. CTRL during low-flow ischemia and reperfusion. Pi was significantly increased in HFS compared with CTRL only during reperfusion. pHi was similar in both groups during the whole protocol. * $p<0.05$ and † $p<0.01$ vs. CTRL (Two-way ANOVA).
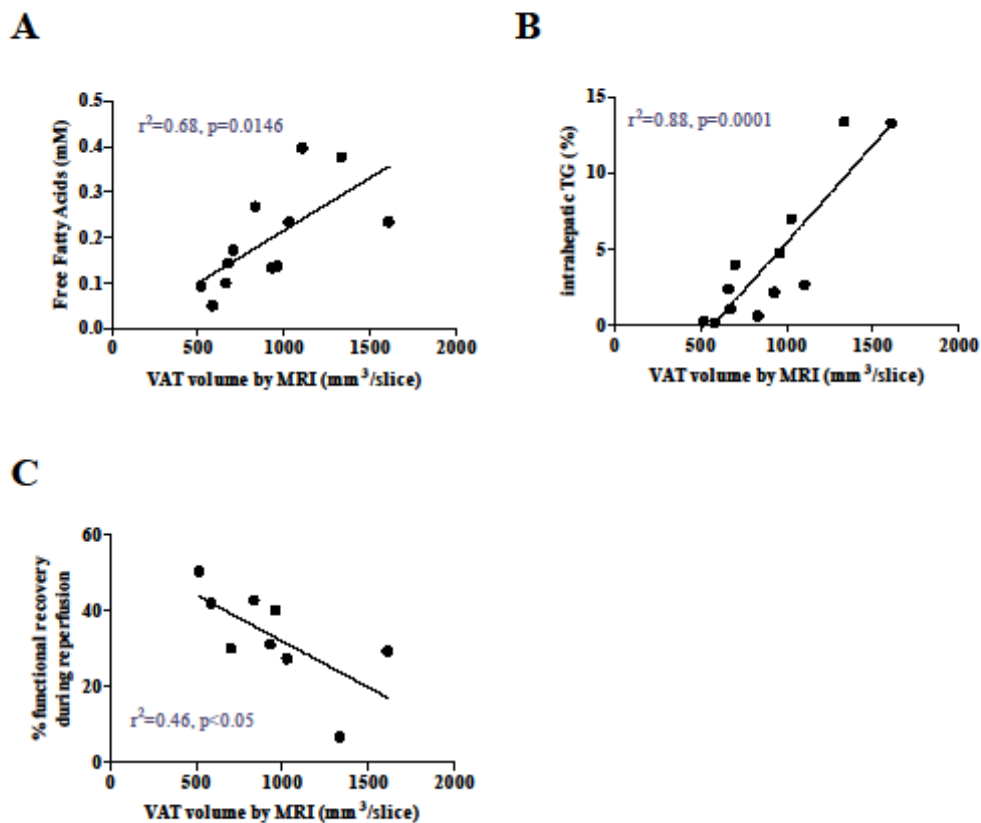
Figure 5

Figure 5: Biochemical analysis in freeze-clamped hearts at the end of ischemia-reperfusion injury. Determination of protein expression of total eNOS (A), P-eNOS (B), eNOS dimer-to-monomer ratio (C) and determination of S-Glutathionylation of total (D) and eNOS (E) proteins by western blot. Data are means ± SEM and t-test was used for all the

parameters. No difference was found between groups for expression of eNOS, and P-eNOS; eNOS uncoupling was significantly higher in HFS vs. CTRL. No difference was found between groups regarding eNOS, P-eNOS expression and S-Glutathionylation of eNOS. The ratio eNOS d/m was significantly decreased in HFS vs. CTRL, indicating eNOS uncoupling. S-Glutathionylation of total proteins was also decreased in HFS vs. CTRL. * p< 0.05 vs. CTRL; † p< 0.05 vs. CTRL.

Figure 6

A

B

C

Figure 6: Correlation analysis between imaging and outcomes. Plasma FFAs (A) and hepatic TG content (B) were correlated to the amount of VAT measured by MRI. Percent of functional recovery during reperfusion was also correlated to the amount of VAT (C).

Figure 7
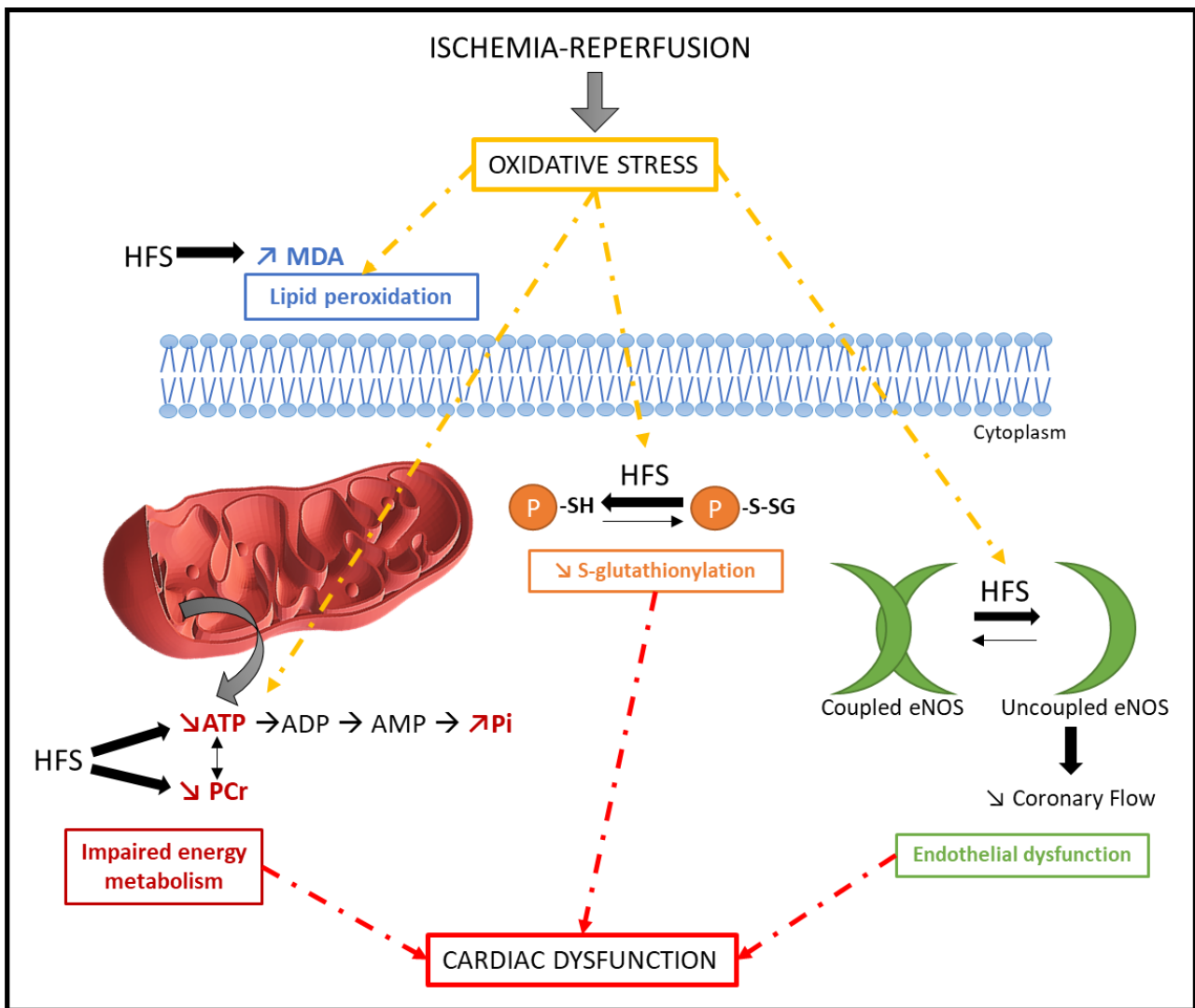
Figure 7: Potential mechanisms involved in the lower tolerance to ischemia-reperfusion in prediabetic female rats. High-fat high-sucrose diet (HFS) increased sensitivity to ischemia-reperfusion injury *ex vivo*. Oxidative stress was exacerbated, with higher MDA level, eNOS uncoupling and lower protection mechanism by S-Glutathionylation in female rat hearts. It might explain the impaired energy metabolism and endothelial function leading to cardiac dysfunction in female gender. Ⓟ: Protein; MDA: Malondialdehyde.

Supplementary material

MRI/MRS investigations

Animals were placed prone on an actively decoupled surface coil (diameter 30mm, Rapid Biomedical, Rimpar, Germany) used for radiofrequency reception. The cardiac region of the thorax was placed at the isocenter of the coil. For assessment of the amount of visceral and subcutaneous adipose tissue in the body the proton volume resonator was used for both radiofrequency transmit and receive. Respiration was monitored using a pressure sensor connected to an air-filled balloon positioned under the rat abdomen. Body temperature was maintained at 37°C using a warming blanket positioned on the back of the animal. The Electrocardiogram (ECG) signal was monitored by two subcutaneous electrodes placed on the upper limbs of the rats. The electrodes were connected to an ECG trigger unit (Rapid Biomedical, Rimpar, Germany) to estimate the heart rate (HR) and to trigger the MR sequences.

Myocardial function and mass

We acquired strictly perpendicular slices in two- and four-chamber long-axis orientation and short-axis orientation at mid-ventricular level (FLASH, field of view, 4 x 4 cm²; slice thickness = 2 mm; matrix size = 128 x 128; TR = 5.1 ms; TE = 1.2 ms; 45 phases per cardiac trigger). Image post processing was performed using an in-house developed program running under an IDL environment (Interactive Data Language, ITT Visual Solutions, Boulder, CO, USA). Left ventricular volumes were determined using an ellipsoid model. Endocardial and epicardial areas were manually delineated on short-axis images, with ventricular lengths determined from four-chamber long-axis views in diastole and systole respectively. End-diastolic volume (EDV), end-systolic volume (ESV), stroke volume (SV), left ventricular ejection fraction (LVEF), mean wall thicknesses in diastole (Wtdia) and systole (Wtsys), and systolic wall thickening (sWtn) were calculated from the volume measurements. Cardiac output (CO) was calculated as CO = HR x SV, and Cardiac Index (CI) = CO / Body weight.

Myocardial perfusion

An ECG and respiration-gated Look-Locker gradient-echo flow-sensitive alternating inversion recovery ASL technique was used to acquire two T1 maps from a single short-axis slice placed at the ventricular mid-level, one after a slice selective inversion pulse and one

after global inversion pulse. The following parameters were used: field of view = 4 x 4 cm²; slice thickness = 3 mm; matrix size = 128 x 64; train of 50 gradient echoes; flip angle = 12°. Image analysis was performed using a home-made program running under IDL environment which generated absolute myocardial blood flow (MBF) maps. MBF, expressed in mL/g/min, was determined as average of pixel values in manually delineated regions of interest in the entire left ventricular myocardium on the corresponding MBF maps.

Cardiac and hepatic TG

The measurement of TG fraction with MRI has been previously validated in our laboratory and was correlated with TG content measured by biochemical analyses.

Voxels were positioned using the short-axis and four-chamber view cine scans as reference. The volume of interest had a size of 1 x 1 x 2 mm^3 and was placed in the basal region of the septum. Acquisitions were done in the systolic phase. The following parameters were used: number of averages (NA) = 512, repetition time equal to the respiratory interval (about 800ms). A second scan was acquired to obtain an unsaturated water peak as reference (TR = 5 s; NA = 64). Molecular content of water was quantified by integration of the resonances at 4.7 ppm and triglycerides at 1.3 ppm in time domain (AMARES fitting). In the liver, a larger voxel size (2 x 2 x 2 mm3) was used to reduce scan time. It was placed in the anterior part of the liver. Parameters were TR = Respiratory interval (about 800ms) and NA = 128. For the reference scan parameters were TR = 5 s and NA = 32. Liver TG were quantified using PRESS with respiratory gating only.

VAT and SCAT

For a quantitative map of adipose tissue distribution, whole-body scanning was performed. Sixty-four contiguous axial imaging slices were selected across the animal body length excluding the tail. Magnetic resonance images of these slices were recorded using a high-resolution three-dimensional (turbo spin echo) sequence with the following parameters: TE = 5.543 ms; effective TE = 88.69 ms; TR = 350 ms; NA = 2; field of view = 80 x 60 x 70 mm^3; matrix size = 128 x 128 x 64. MR data were processed using a custom-written analysis program developed with the IDL software. Quantification of both VAT and SCAT was performed using an automatic segmentation method based on a pixel intensity analysis of MR images.

Isolated perfused heart

Energy metabolism assessment by ^{31}P magnetic resonance spectroscopy – Quantification of phosphorus metabolites and determination of intracellular pH.

^{31}P spectra were obtained by accumulating 328 free induction decay signals acquired for 4 minutes (flip angle 45°, repetition time 0.7 s, spectral width 4500 Hz, 2,048 data points). Quantification of the signal integrals was carried out using an external reference containing an aqueous solution of 0.6 mM phenylphosphonic acid.

Biochemical analyses in freeze-clamped heart

Apoptosis

The expression of cleaved caspase-3 (active form) was determined in heart homogenates by Western Blot. Samples (50 µg) were run in Tris-Glycine-SDS with 4-20% gradient gel (Bio-Rad, Mini-PROTEAN TGX, Precast Gels) and transferred to pure nitrocellulose membrane (0.45 µm, Bio-Rad) with a semi-dry transfer device (Transblot SD system, Biorad). After blocking, membranes were incubated overnight at 4°C with primary anti-rabbit antibody against Caspase-3 (1/1000; Cell Signaling Technology, Inc, USA) and secondarily with HRP-conjugated anti-rabbit antibody (1/2000; Santa Cruz Biotech).

NO pathway

The expression of total eNOS, eNOS -PSer1177 and eNOS dimer-to-monomer ratio (eNOS d/m) were determined in heart homogenates by Western Blot. Proteins were separated by gel electrophoresis and transferred onto PVDF membranes. After blocking, membranes were incubated overnight at 4°C with primary antibody: anti-mouse eNOS (1/1000 for eNOS and eNOS d/m, BD Biosciences), anti-mouse eNOS-Pser1177 (1/1000, BD Biosciences); and secondarily with HRP-conjugated antibody.
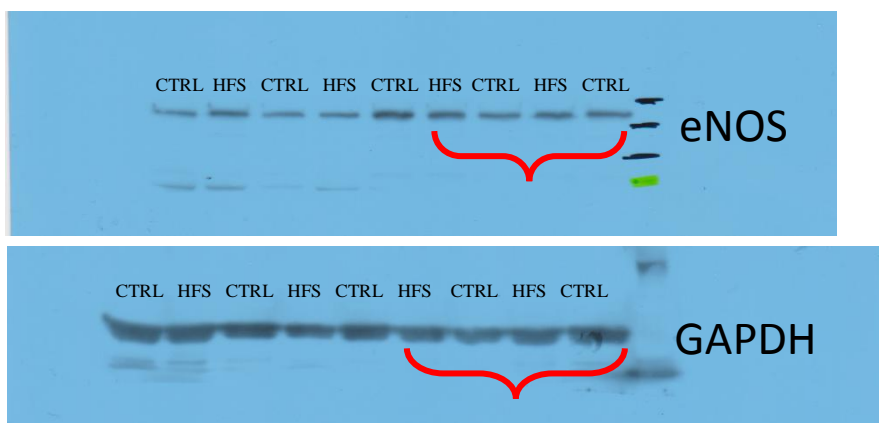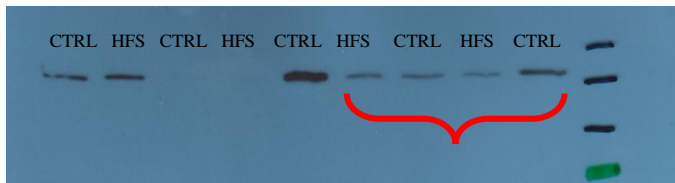
Post-translational modification of proteins

S-Glutathionylation of proteins was evaluated by Western Blot. Protein samples (80μg) were run in SDS-PAGE (8%) and transferred to PVDF membrane. After blocking, membranes were incubated with primary anti-mouse antibody against Glutathione (1/500; Santa Cruz Biotech) and secondarily with HRP-conjugated antibody (1/5000; BD Bioscience). eNOS S-Glutathionylation was determined by stripping and incubating the same membrane with primary anti-mouse antibody against eNOS as described above.

Table 2: Cardiac function parameters measured by MRI after 5 months of diet in CTRL and HFS. Results are expressed as means ± SEM.
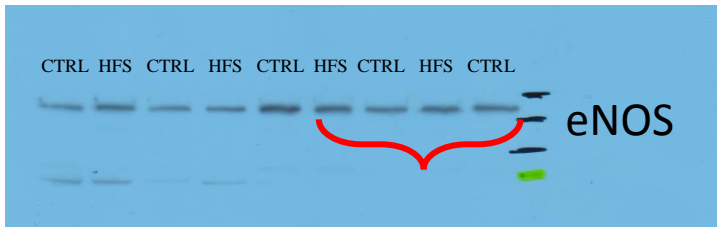
	CTRL	HFS
LVVdia (μL)	890 ± 26	948.9 ± 34.5
EDV (μL)	403.6 ± 16.5	397 ± 14
LVVsys (μL)	666.5 ± 20.9	719 ± 32
ESV (μL)	114 ± 9	98.1 ± 11.6
SV (μL)	289.6 ± 9.9	298.5 ± 7.3
EF (%)	72 ± 1	76 ± 2
CO (mL/min)	109.3 ± 5.7	128.4 ± 3.8
CI (μL/min/g)	408.7 ± 23.3	453.9 ± 31.3

Western Blot used for figure 5

CTRL HFS CTRL HFS CTRL HFS CTRL HFS CTRL

P-eNOS

CTRL HFS CTRL HFS CTRL HFS CTRL HFS CTRL

eNOS

eNOS dimer (280 kDa)
eNOS monomer (140 kDa)

CTRL HFS CTRL HFS CTRL HFS CTRL HFS

eNOS S-Glut

130 kDA
95 kDA
72 kDA

CTRL HFS CTRL HFS CTRL HFS CTRL HFS CTRL
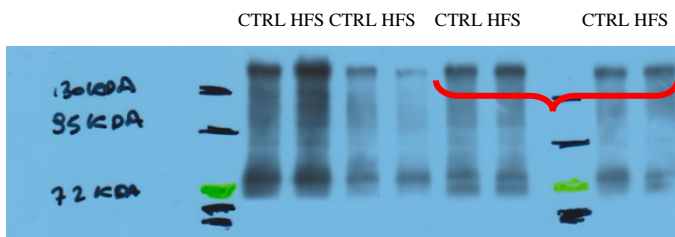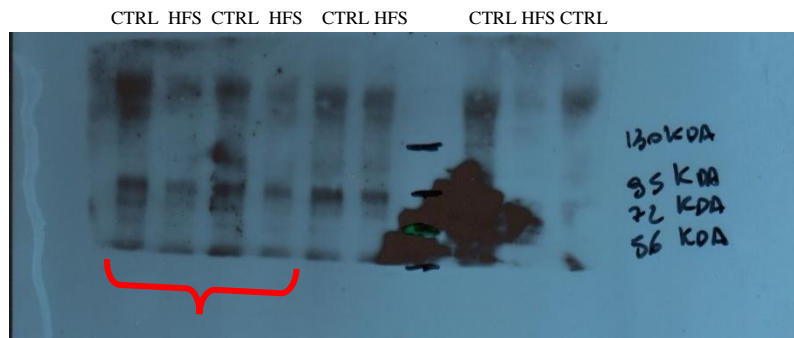
Glutathionylated proteins

130 kDA
95 kDA
72 kDA
56 kDA